ELSEVIER

Journal of Hazardous Materials B135 (2006) 280–295

Journal of Hazardous Materials

www.elsevier.com/locate/jhazmat

Trivalent chromium removal from wastewater using low cost activated carbon derived from agricultural waste material and activated carbon fabric cloth

Dinesh Mohan *, Kunwar P. Singh, Vinod K. Singh

Environmental Chemistry Division, Industrial Toxicology Research Centre, Post Box No. 80, Mahatma Gandhi Marg, Lucknow 226001, India

Received 23 October 2005; received in revised form 17 November 2005; accepted 23 November 2005
Available online 25 January 2006

Abstract

An efficient adsorption process is developed for the decontamination of trivalent chromium from tannery effluents. A low cost activated carbon (ATFAC) was prepared from coconut shell fibers (an agricultural waste), characterized and utilized for Cr(III) removal from water/wastewater. A commercially available activated carbon fabric cloth (ACF) was also studied for comparative evaluation. All the equilibrium and kinetic studies were conducted at different temperatures, particle size, pHs, and adsorbent doses in batch mode. The Langmuir and Freundlich isotherm models were applied. The Langmuir model best fit the equilibrium isotherm data. The maximum adsorption capacities of ATFAC and ACF at 25 °C are 12.2 and 39.56 mg/g, respectively. Cr(III) adsorption increased with an increase in temperature (10 °C: ATFAC—10.97 mg/g, ACF—36.05 mg/g; 40 °C: ATFAC—16.10 mg/g, ACF—40.29 mg/g). The kinetic studies were conducted to delineate the effect of temperature, initial adsorbate concentration, particle size of the adsorbent, and solid to liquid ratio. The adsorption of Cr(III) follows the pseudo-second-order rate kinetics. From kinetic studies various rate and thermodynamic parameters such as effective diffusion coefficient, activation energy and entropy of activation were evaluated. The sorption capacity of activated carbon (ATFAC) and activated carbon fabric cloth is comparable to many other adsorbents/carbons/biosorbents utilized for the removal of trivalent chromium from water/wastewater.

Keywords: Adsorption; Low cost adsorbents; Chromium removal; Trivalent chromium; Activated carbons; Utilization of agricultural waste materials; Wastewater treatment; Tannery wastewater

1. Introduction

Chromium compounds are widely used by modern industries, resulting in large quantities of this element being discharged into the environment. Some of the main used of chromium compounds is (a) plastic coatings, (b) electroplating of metal for corrosion resistance, (c) leather tanning and finishing, and (d) in pigments and for wood preservative. Thus, chromium occurs in wastewater resulting from these operations in both trivalent and hexavalent forms. Chromium has been found in at least 115 of 1300 National Priorities List sites identified by the EPA. Chromium exists in nature mainly in two oxidation states, +3 and +6. It is bio element in +3 state but mutagenic in +6 state. The hydrolysis behavior of Cr(III) is complicated and it produces mononuclear species $CrOH^{2+}$, $Cr(OH)_2{}^{+}$, $Cr(OH)_4{}^{-}$, neutral species $Cr(OH)_3{}^{0}$, and poly-nuclear species $Cr_2(OH)_2$ and $Cr_3(OH)_4{}^{5+}$. The drinking water guideline recommended by Environmental Protection Agency (EPA) in US is 100 μg/l. The legal discharge limit of Cr(III) varies from 0.5 mg/l (in surface water) to 2.0 mg/l (in sewers) depending on the processing, country, and wastewater treatment methods [1].

Tanning is one of the oldest and fastest growing industries in India. There are about 2161 tanneries in India excluding cottage industries, which processed 500,000 tonnes of hides and skins annually [2]. In 2161 tanneries in India, a total of 314 kg skin is processed per year. A total annual discharge of wastewater from these tanneries is 9,420,000 m^3 [2]. Numerous treatment methods such as Ion exchange [3–5], reduction [6], chemical precipitation [7], membrane separations [8,9], electrochemical precipitation [10], photocatalytic reduction [11], adsorption [12–14], and biosorption [15,16] have been developed for chromium remediation. The precipitation, oxidation/reduction,

* Corresponding author. Tel.: +91 522 2508916; fax: +91 522 2628227.
E-mail address: dm_1967@hotmail.com (D. Mohan).

0304-3894/$ – see front matter © 2005 Elsevier B.V. All rights reserved.
doi:10.1016/j.jhazmat.2005.11.075

lime neutralization have traditionally been the most commonly used. Although these technologies are quite satisfactory in terms of purging chromium from water but they (except few) produce solid residue (sludge) containing toxic compounds whose final disposal is generally by land filling with relative high costs and still a possibility of ground water contamination. Nevertheless, many of these approaches are marginally cost-effective or difficult to implement in developing countries. Therefore, the need exists for a treatment strategy that is simple, robust, and that addresses local resources and constraints. Sorption (adsorption as well as biosorption) may be an effective and versatile method for removing chromium, particularly when combined with appropriate regeneration steps. This solves the problems of sludge disposal and renders the system more economically viable, especially if low cost adsorbents are used.

Many activated carbons are available commercially but very few of them are selective for heavy metals and are also expensive. Despite the use of carbon [17–20], it is an expensive treatment processes for chromium bearing water/wastewater and improved and tailor made materials are needed for these demanding applications. Investigators have studied less expensive materials for the removal of chromium from water such as cellulose adsorbent [21], sugar beet pulp [22], polyacrylonitrile fibers [23], alginate beds [24], carbon developed from waste materials [12,13,25], biosorbents [15,26,27], bagasse fly ash [28], blast furnace waste [12], red mud [29], agricultural waste [30], and zeolites [31]. Pollard et al. [32], Radovic et al. [33], and Gupta and Ali [34] reviewed low cost adsorbents used for the remediation of toxic substances from water. However, these adsorbents were never fully explored. This calls for a research effort to develop an industrially viable, cost-effective, and environmentally compatible technology for the removal of chromium from wastewater. For quite some time we are involved in developing some low cost activated carbons/adsorbents for the removal and recovery of organics/metal ions from wastewater [2,35–39]. Recently we have reported a variety of activated carbons for hexavalent chromium remediation [2]. Continuing our activities in this direction, we have derived a low cost activated carbon from coconut shell fibers and used for the removal of trivalent chromium from synthetic tannery wastewater. A commercially available activated carbon fabric cloth (ACF) was also investigated for the removal of trivalent chromium from water/wastewater.

2. Materials and methods

2.1. Reagents and equipments

All chemicals were AR grade. Stock solution of test reagent was made by dissolving $Cr(NO_3)_3{\cdot}9H_2O$ in double distilled water. The pH measurements were made using a Metrohm pH meter. Test solutions pHs were adjusted using reagent grade dilute H_2SO_4 (0.1N) and NaOH (0.1N). The aqueous total chromium concentrations in the samples were determined by atomic absorption (Perkin-Elmer 3100) spectrophotometer with an air-acetylene flame using Cr-hallow cathode lamp. Agitation of adsorbent–adsorbate was carried out on a thermostatic shaking assembly (model NSW-133, India).

Activated carbon was characterized in terms of chemical composition by carrying out the proximate and elemental analysis and also texturally by gas adsorption, mercury porosimetry, and helium and mercury density measurements. Infrared spectra were obtained on carbon in KBr disks from 500 to 4000 cm^{-1} using a Perkin-Elmer spectrophotometer. XRD line profile analysis was performed using a Philips powder X-ray diffractometer. Cu Kα ($\lambda = 1.54$ Å) radiation was used with a scanning step of 0.05 Å from $10^\circ < 2\theta < 60^\circ$. The scanning electron microscopy was performed using a Philips XL-20 electron microscope.

The values of the BET specific surface area (S_{BET}) and pore volumes (micropore volume, V_{mi} and W_o; mesopore volume, V_{me} and $V_{me\text{-}p}$; macropore volume, $V_{ma\text{-}p}$; and total pore volume, V_T) were determined using Quantachrome surface area analyzer model Autosorb-1. The mercury porosimetries have been carried out with a Quantachrome porosimeter model Autoscan-60. The mercury density has been determined as usual, when carrying out the mercury porosimetry experiments. The helium density has been measured using a Quantachrome Stereopycnometer.

The chemical constituents of activated carbon were analyzed following the standard methods of chemical analysis [2,40].

2.2. Quality assurance/quality control

To establish the accuracy, reliability, and reproducibility of the collected data all the batch isotherm tests were replicated twice and the experimental blanks were run in parallel. Blanks were run and corrections were applied if necessary. Multiple sources of National Institute of Standard and Technology (NIST) traceable standards were used for instrument calibration and standard verification. All jars, conical flasks and containers used in the study were prepared by being soaked in a 5% HNO_3 solution for a period of 3 days before being double rinsed with distilled, deionized water, and oven dried. All the observations were recorded in triplicate and average values are reported.

Non-linear regression analysis was applied to each set of data point. A correlation coefficient (R^2) and a probability value (p) represent the "goodness of fit" of the Freundlich or Langmuir model to the data was obtained by the linear as well as non-linear regression program using Sigma Plot V6.0 for windows, SPSS Inc., Chicago, IL, USA.

2.3. Adsorbent development

Coconut shell fibers (agricultural waste materials) that often presents serious disposal problem for local environment were collected locally from Lucknow (U.P.), India. Activated carbon was prepared by treating one part of coconut shell fibers with two parts (by weight) of concentrated sulfuric acid and keeping the mixture in an oven maintained at 150–165 °C for a period of 24 h. The carbonized material was washed well with double distilled water to remove the free acid and dried at 105–110 °C for 24 h. Dried coconut shell fibers were subjected to thermal activation at different temperatures, viz., 200, 400, 600, and 800 °C for 1 h in an inert atmosphere. The temperature and time were

optimized by observing the surface properties of the activated products obtained. The products obtained at temperatures higher or lower than 600 °C exhibited less adsorption capacities. The activation was carried out under closely controlled conditions to obtain optimum properties. The products so obtained were sieved to the desired particle sizes such as 30–200, 200–250, and 250–300 mesh. Finally, the product was stored in a vacuum desiccator until required. The developed carbon is designated as ATFAC (activated carbon derived from acid treated coconut shells). The carbon having 30–200 mesh size was used in both the sorption and kinetic studies unless otherwise stated.

For comparative evaluation, a commercially available activated carbon fabric cloth was used for the removal of Cr(III). The ACF was obtained from HEG Limited, Mandideep, Bhopal, India. According to the manufacturer, the activated carbon fabric was prepared by carbonization of precursor in an inert atmosphere after due chemical treatment. Activation is carried out under closely controlled process parameters to get optimum properties.

2.4. Sorption procedure

Batch sorption studies were performed to obtain rate and equilibrium data due to their simplicity. Different temperatures, particle sizes, adsorbent doses were employed to obtain equilibrium isotherms and data required for design and operation of column reactors to treat Cr(III) bearing wastewater. Conical flasks (100 ml) employed for the isotherm studies were filled with 50 ml solution of Cr(III). Concentrations (1–100 mg/l) were used based on extensive preliminary investigations and in accord with chromium concentrations found in industrial effluents. Solution pH and temperature was adjusted. A known amount of either adsorbent (0.1 g) was added to each flask followed by intermittent agitation for specified times up to a maximum of 48 h. No further uptake occurred between 48 and 72 h. All equilibrium tests were conducted for 48 h. After this period the solutions were filtered using Whatman no. 42 filter paper and the remaining concentrations of chromium were determined. The effect of pH on Cr(III) adsorption was studied over a broad pH range of 2–6. The sorption studies were also carried out at different temperatures, i.e. 10, 25, and 40 °C to determine the effect of temperature. Adsorption of Cr(III) was also studied at different doses of adsorbent and particle sizes. The concentration of Cr(III) retained in the adsorbent phase is calculated as the difference between the original concentration of the solution and the measured concentration in solution after equilibrium. The mass balance can be expressed as

$$W(q_e - q_0) = V(C_0 - C_e) \quad (1)$$

when $q_0 = 0$, Eq. (1) becomes equivalent to

$$q_e = \frac{(C_0 - C_e)V}{W} \quad (2)$$

where q_0 and q_e are initial and equilibrium concentrations, respectively, of chromium on adsorbents (mg/g), C_0 and C_e the initial and equilibrium concentrations (mg/l) of Cr(III) in solution, V the volume (l), and W is the weight (g) of the adsorbent.

2.5. Kinetic studies

Successful application of adsorption processes demands the development of cheap, non-toxic, available adsorbents of known kinetic parameters, and sorption characteristics. Foreknowledge of optimal conditions would enable a better process design and modeling. Thus, the effect of contact time, amount, adsorbent particle size, and adsorbate concentration were studied. At desired temperatures, predetermined amounts of adsorbent were added to stoppered flasks (100 ml) containing 50 ml solutions of chromium in a thermostatic shaking assembly. The solutions were agitated. At predetermined intervals adsorbent was separated and analyzed for Cr(III) uptake. The Cr(III) adsorbed was calculated using Eq. (2).

3. Result and discussions

3.1. Characterization

The prepared carbon (1.0 g) was stirred with deionized water (100 ml, pH 6.8) for 2 h and left for 24 h in an airtight-stoppered conical flask. After 24 h, an decrease in the pH (5.80) was recorded confirming that carbon is of L type [2,35,36,37]. The carbon is quite stable in water, salt solutions, dilute acids, dilute bases, and organic solvents. The specific surface area of the carbon was evaluated from the N_2 isotherms by applying the Brunaeur, Emmett, and Teller (BET) equation at a relative pressure (p/p_0) of 0.35 and a_m equal to 16.2 Å (a_m is the average area covered by a molecule of N_2 in completed monolayer). From the aforesaid isotherms as well, the micropore volume has been obtained by taking it to be equal to the volume of N_2 adsorbed at $p/p_0 = 0.10$ (V_{mi}) and also by applying the Dubinin–Radushkevich equation (W_0). V_{mi} and W_0 are expressed as liquid volumes. The volumes of mesopores (V_{me}) and macropores (V_{ma}) have been derived from the curves of cumulative pore volume (V_{cu}) against pore radius (r) (mercury porosimetry): $V_{me} = V_{cu}$ (at $r = 20$) $- V_{ma}$ and $V_{ma} = V_{cu}$ (at $r = 250$ Å). The total pore volume has been calculated by making use of the expression: $V_T = 1/\rho_{Hg} - 1/\rho_{He}$, ρ_{Hg} and ρ_{He} being the mercury and helium densities, and also by adding up V_{mi}, V_{me}, and V_{ma}. The values of S_{BET}, V_{mi}, W_o, V_{me}, ρ_{Hg}, ρ_{He}, V_T, and V'_T are listed in Table 1.

The X-ray diffraction analysis of activated carbon did not show any peak indicating amorphous nature of the carbon prepared from coconut shell fibers.

The identification of various forms of different constituents in ATFAC activated has been done with the help of IR spectra (Fig. 1). The IR spectrum of activated carbon indicated weak and broad peaks in the region of 3853–453 cm^{-1}. Approximate FT-IR band assignment indicated the presence of carbonyl, carboxyls, lactones, and phenols. The 1800–1540 cm^{-1} band is associated with C=O stretching mode in carbonyls, carboxylic acids, and lactones, while 1440–1000 cm^{-1} band was assigned to the C−O stretching and O−H bending modes such as phe-

Table 1
Characteristics of prepared activated carbon and activated carbon fabric cloth

Activated carbon (ATFAC)		Activated carbon fabric cloth (ACF)	
Properties	Values	Properties	Values
pH	5.80	Surface area (S_{BET}) (m^2/g)	1565
Ash (%)	7.23	Pore volume (cm^3/g)	0.65
C:H:N (%)	76.38:1.95:0.38	Effective pore size (Å)	<8.0
S_{BET} (m^2/g)	512	Thickness (mm)	7–9
V_{mi} ($cm^3\ g^{-1}$)	0.17	Density (gm/cm^3)	0.2–0.7
W_o ($cm^3\ g^{-1}$)	0.18	Decomposition temperature (°C)	>500
V_{me} ($cm^3\ g^{-1}$)	0.07	Width (cm)	60/87
V_{ma} ($cm^3\ g^{-1}$)	0.29	Texture	Plain
ρ_{Hg} ($g\,cm^{-3}$)	1.65	pH	7.0
ρ_{He} ($g\,cm^{-3}$)	0.84	Hydrogen percentage	0.80
V_T ($cm^3\ g^{-1}$)	0.58	Carbon percentage	80
V'_T ($cm^3\ g^{-1}$)	0.53		

nols and carboxylic acids. The assignment of a specific wave number to a given functional group was not possible because the absorption bands of various functional groups overlap and shift, depending on their molecular structure and environment. Shifts in absorption positions may be caused by factors such as intra-molecular and intermolecular hydrogen bonding, stearic effect, and degree of conjugation. For instance, within its given range, the position of C=O stretching band (common to carbonyls, carboxylic acids, and lactones) is determined by many factors. These include: (i) the physical state, (ii) electronic and mass effects of neighboring substituents, (iii) conjugation, (iv) hydrogen bonding, and (v) ring strain. The IR absorption bands of oxygen groups on the surface of solid GAC are likely to be affected by some or all of the factors listed above. Although some inference can be made about the surface functional groups from IR spectra, the weak and broad band do not provide any authentic information about the nature of surface oxides.

Scanning electron microscopy of ATFAC [2,35,36,37] at different magnifications revealed the surface texture and different levels of porosity in the prepared activated carbon under study. It was concluded that there were considerable small cavities, cracks and attached fine particles over the activated carbon surface, forming a system of complicated pore networks.

On the other hand, activated carbon fabric cloth is synthetic material manufactured from an array of uniform polymeric substrates, including polyacrylonitrile, pitch-based polymers, and phenolic-based resins [41]. These materials can be used to produce ACFs with uniform and continuous pore structures; in addition, they contain very low amounts of inorganic impurities compared with conventional activated carbon feed stocks. ACF uses chiefly cellulose or acrylic precursors. Cellulose based precursor (for example, from viscose rayon) tend to have a very low yield and not too good mechanical properties. Acrylic-based ACF is increasing becoming a major product in all aspects of chemical filtration.

The production of ACF involves stabilizing the acrylic precursor in the same way as by structural carbon fibers, in air up to 300 °C. The resulting oxidized fiber can be directly activated or more usually made into a fabric through conventional textile means (felting, spinning, and weaving or knitting). The oxidized acrylic cloth is then activated, this involves heating the fabric to a temperature of up to 1300 °C not in an inert atmosphere like in structural carbon fiber but in an oxidizing atmosphere such as CO_2 or H_2O (steam). The action of the oxidizing agent causes a tremendous attack on the surface of the fibers, this induces a huge surface area and a porous surface which the size and configuration of the pores influence

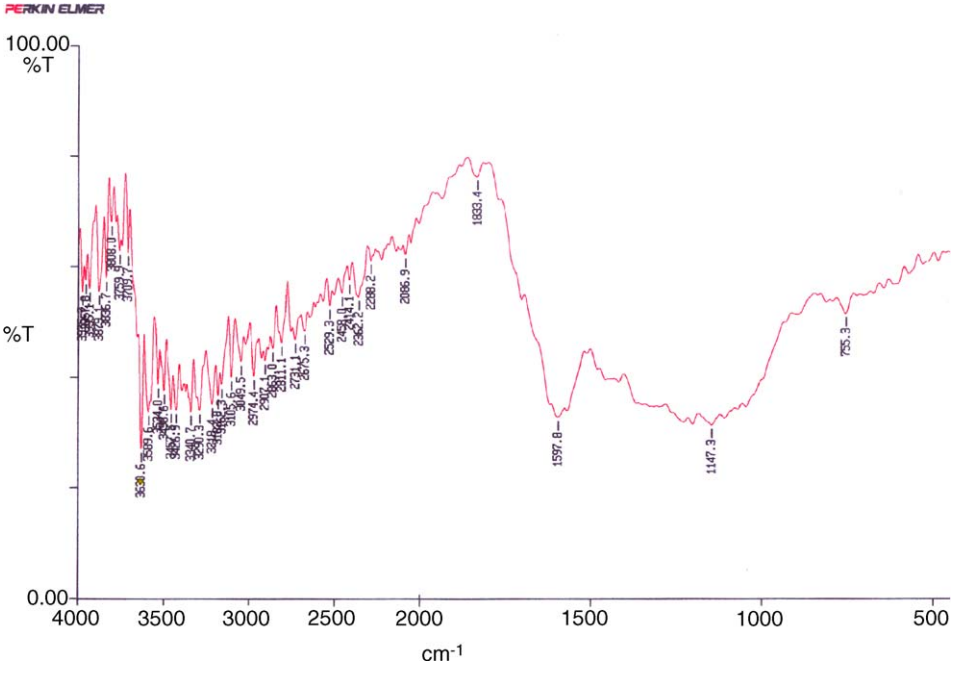

Fig. 1. IR spectrum of ATFAC.

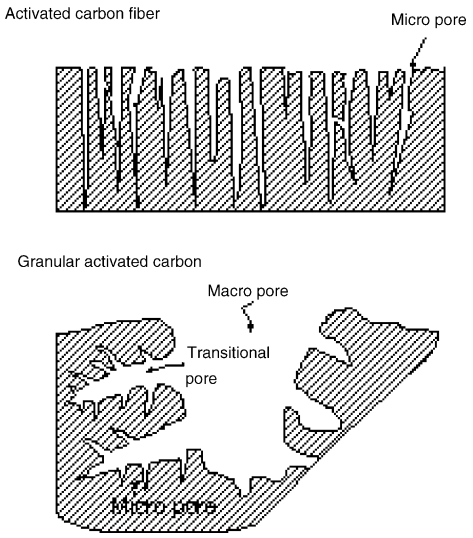

Fig. 2. Activated carbon and activated carbon fabric cloth (ACF) structures.

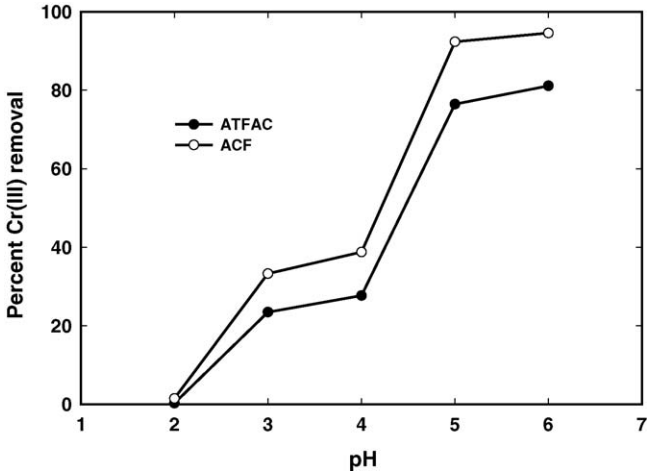

Fig. 3. Effect of pH on the adsorption of Cr(III) by ATFAC and ACF at 25 °C and adsorbate concentration of 50 mg/l.

greatly the power of the carbon atoms, on the surface to act as chemical "hooks" to attach to many chemical substances which may pass through the ACF filter. Basically ACF carbon is a form of graphite, free of nitrogen, hydrogen, halogens, sulfur, or oxygen. The activated carbon structure allows for high porosity as millions of pore sizes, from visible cracks and crevices to inlets of molecular dimensions all allowing for adsorption. The activated carbon employed for purification purpose usually contained macro- (10–30%), meso- (20–40%), and micropores (40–50%) (radii >50, 50–2, and <2 nm, respectively), however the activated carbon cloth can be prepared with micropores only or with a mixture of pores. The former version of charcoal cloth is of particular interest because its pore sizes distribution differs from that of activated carbon as shown in Fig. 2.

These materials can be used molecules/atoms of pollutants have an affinity towards activated carbon fabric surface by physical adsorption at low temperatures. In physical adsorption there is a van der Waals interaction, having long range, but weak forces. Molecule of pollutant bouncing across the activated carbon fabric surface gradually looses its energy and finally comes to rest on it. Due to weak bonds in the physical adsorption molecules can be removed from the activated carbon fabric surface by giving heat input. This property is utilized in regenerating activated carbon fabric. The various properties of the activated carbon fabric cloth are provided in Table 1.

3.2. Equilibrium studies

Cr(III) in aqueous solution forms different species at various pHs [19]. The speciation diagram for chromium(III) can be obtained using the following reactions and equilibrium constants [25]:

$$Cr^{3+} + H_2O \leftrightarrow Cr(OH)^{2+} + H^+ \quad (\log K = -4)$$

$$Cr^{3+} + 2H_2O \leftrightarrow Cr(OH)_2{}^+ + 2H^+ \quad (\log K = -9.65)$$

$$Cr^{3+} + 4H_2O \leftrightarrow Cr(OH)_4{}^- + 4H^+ \quad (\log K = -27.4)$$

$$Cr^{3+} + 3H_2O \leftrightarrow Cr(OH)_{3(s)} + 3H^+ \quad (\log K = -12)$$

The first reaction generates $Cr(OH)^{2+}$ and protons which contribute to the increased acidity of Cr(III) solution. If Cr^{3+} is adsorbed, the first reaction proceeds to the left, leading to the depletion of protons and hence a rise in pH. In contrast, if $Cr(OH)^{2+}$ adsorbs onto the adsorbent, the reaction proceeds to the right and the solution becomes more acidic. However, the pH of a solution may also change due to the release and/or uptake of protons. Thus, $Cr(OH)_2{}^+$ species is dominant at pH values between 6 and 8 while $Cr(OH)^{2+}$ and Cr^{3+} predominant in more acidic conditions. $Cr(OH)_4{}^-$ and $Cr(OH)_{3(s)}$ are most likely to be found in alkaline water.

The removal of chromium as a function of pH was investigated over a pH range of 2–6 (Fig. 3). It is clear that sorption of trivalent chromium species increased with increase in solution pH from 2 to 6.0. Studies were not performed beyond 6.0 due to the possibility of Cr(III) precipitation [23,42]. Rivera-Utrilla and Sanchez-Polo [43] calculated the distribution of Cr(III) species in aqueous solutions at different pH values. At pH 2, almost all the Cr(III) existed as Cr^{3+} cation (hexahydrated), whereas at pH 12 it existed as $Cr(OH)_4{}^-$ anion. At pH 4.0, the predominant species were Cr^{3+} (61.16), $Cr(OH)^{2+}$ (38.60), and $Cr(OH)_2{}^+$ (38.24) while at pH 6.0 the predominant species were $Cr(OH)^{2+}$ (60.61%) and $Cr(OH)_2{}^+$ (38.24%). At pH 2, the amount of Cr(III) adsorbed on ATFAC and ACF is almost zero. The smaller adsorption values observed at low pH have been attributed to the competition between the protons and the Cr(III) for the available binding sites on carbon. The adsorption increases in the range 4–6.0. In this pH range, all Cr(III) species are cationic and the predominant interactions in the adsorption process must have been electrostatic. The maximum adsorption capacities were achieved in a pH range (4–6) at which the carbon surface presented a negative charge and the Cr(III) species were cationic. Thus, the adsorption of Cr(III) is a attractive electrostatic interactions between the ionised acid sites

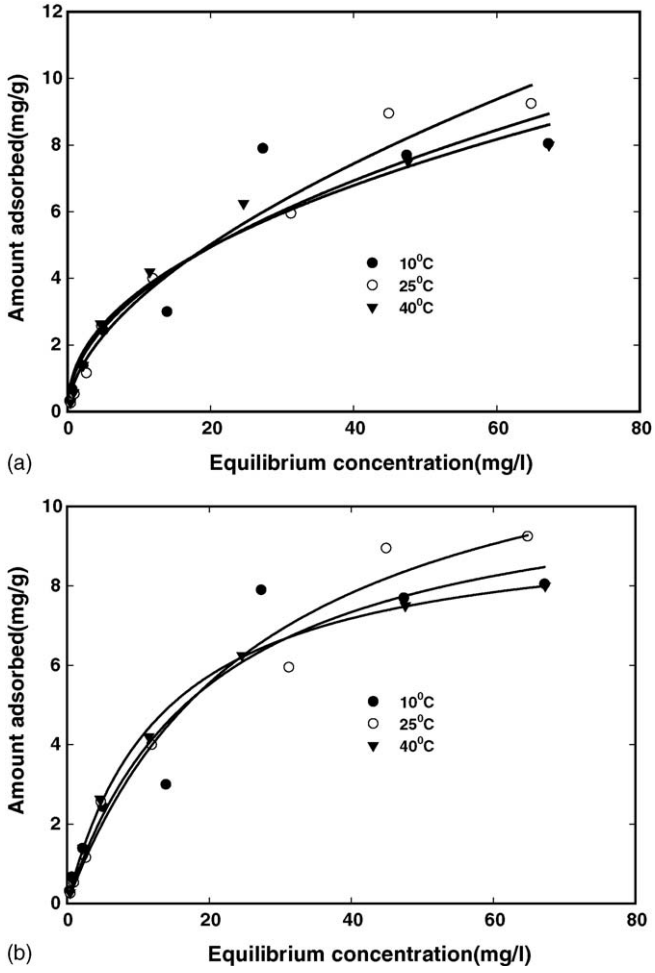

Fig. 4. Adsorption of Cr(III) on ATFAC at different temperatures and at optimum pH. Solid lines represent the fitting of data by (a) Freundlich and (b) Langmuir isotherms.

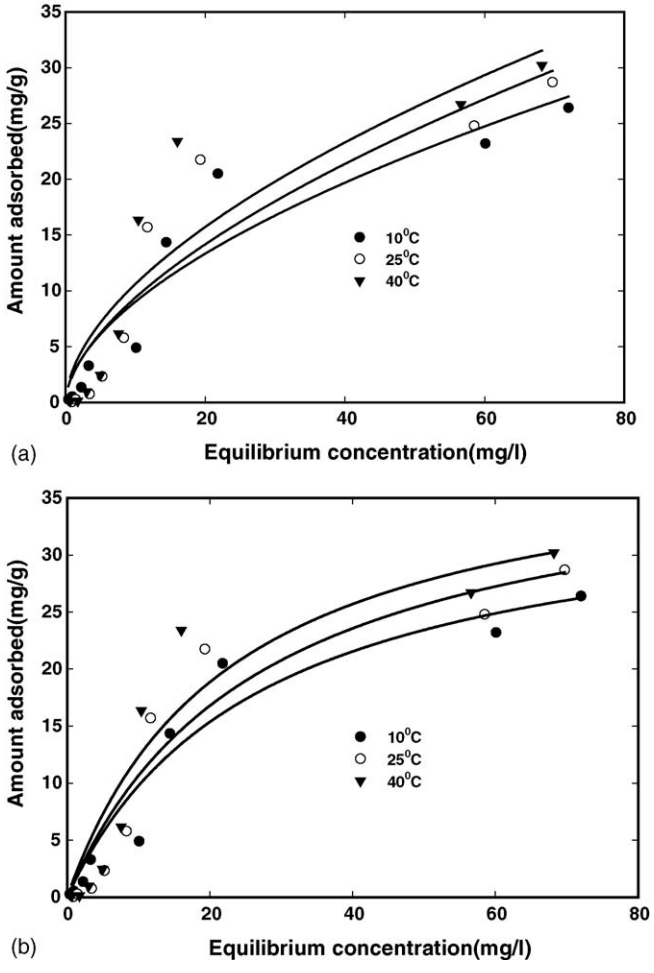

Fig. 5. Adsorption of Cr(III) on ACF at different temperatures and at optimum pH. Solid lines represent the fitting of data by (a) Freundlich and (b) Langmuir isotherms.

on the activated carbon surface and the Cr(III) cations. Leyva-Ramos et al. [19] report that at pH values below 2, Cr(III) was not adsorbed and at pH values above 6.4 Cr(III) was precipitated. Aggarwal et al. [44], studied the adsorption of Cr(III) and Cr(VI) on activated carbons with different degrees of oxidation and concluded that the adsorption of Cr(III) is specifically produced on carboxyl and lactone groups present on the activated carbon surface. Rivera-Utrilla and Sanchez-Polo [43] investigated that at pH values above 7, neutral $Cr(OH)_3$ and anionic $Cr(OH)_4^-$ species begin to appear, reducing the adsorption capacity of these samples by preventing ionic interchange and creating repulsive adsorbent–adsorbate interactions. In the present investigation the optimum initial pH chosen for Cr(III) was 5.0, to correlate the removal with adsorption process. Similar types of observations for the Cr(III) adsorption were reported earlier [17,33,45].

The isotherms (data points) for adsorption of the Cr(III) at optimum pH on activated carbon developed from coconut shell fibers and activated fabric cloth are shown in Figs. 4 and 5 at three different temperatures. However, the data points are not very good but still the isotherms are positive, regular, and concave to the concentration axis. In all the cases the uptake of Cr(III) increases with increase in temperature thereby indicating the process to be endothermic in nature.

The increase in adsorption of chromium(III) with temperature is probably a combination of "activated diffusion" plus an increase in surface area caused by oxidation, associated with the observed adsorption of Cr(III) on the surface of carbonaceous materials. Such activated adsorption would widen and deepen the very small micropores, i.e. cause "pore burrowing" and so create more surfaces for adsorption [46]. Thus, the increase in the number of the adsorption sites due to the breaking of some internal bonds near the edge of the particles at higher temperatures resulting the higher adsorption of Cr(III) [46].

The uptake of Cr(III) by ATFAC and ACF is almost 100% at low adsorbate concentrations while it decreases at higher adsorbate concentrations. The adsorption studies were carried out at 10, 25, and 40 °C to determine the adsorption isotherms and the isotherm parameters were evaluated using linear and non-linear Langmuir and Freundlich models as given by Eqs. (3)–(6). Use of linearized equations apparently produces large errors in the parameters. This is related to complication arising from the simultaneous transformation of measurement errors with data.

Table 2
Freundlich isotherm constants for Cr(III) adsorption on ATFAC and ACF at different temperatures

Types of carbons	10 °C			25 °C			40 °C		
	K_F (mg/g)	n	R^2	K_F (mg/g)	n	R^2	K_F (mg/g)	n	R^2
ATFAC	1.14	0.49	0.9131	0.911	0.56	0.9766	1.26	0.45	0.9698
ACF	2.47	0.56	0.9026	2.39	0.59	0.8622	2.87	0.56	0.8415

3.2.1. Langmuir isotherm

The Langmuir equation may be written as

$$q_e = \frac{Q^0 b C_e}{1 + bC_e} \quad \text{(non-linear form)} \tag{3}$$

$$\frac{C_e}{q_e} = \left(\frac{1}{Q^0 b}\right) + \left(\frac{1}{Q^0}\right) C_e \quad \text{(linear form)} \tag{4}$$

where q_e is the amount of solute adsorbed per unit weight of adsorbent (mg/g), C_e the equilibrium concentration of solute in the bulk solution (mg/l), Q^0 the monolayer adsorption capacity (mg/g), and b is the constant related to the free energy of adsorption/desorption ($b\alpha\, e^{-\Delta G/RT}$). High values of b are reflected by the steep initial slope of a sorption isotherm and indicate a high affinity for the adsorbate. In terms of implementations, sorbents with highest possible Q^0 and high b are the most desirable.

3.2.2. Freundlich isotherm

The Freundlich equation may be written as

$$q_e = K_F C_e^{1/n} \quad \text{(non-linear form)} \tag{5}$$

$$\log q_e = \log K_F + \frac{1}{n} \log C_e \quad \text{(linear form)} \tag{6}$$

where q_e is the amount of solute adsorbed per unit weight of adsorbent (mg/g), C_e the equilibrium concentration of solute in the bulk solution (mg/l), K_F the constant indicative of the relative adsorption capacity of the adsorbent (mg/g), and $1/n$ is the constant indicative of the intensity of the adsorption.

The non-linear Freundlich and Langmuir isotherms for the adsorption of Cr(III) on the prepared activated carbons and activated carbon fabric at different temperatures are also presented in Figs. 4 and 5. The solid lines represent the lines of model fits in the wide range of concentrations. The corresponding Freundlich and Langmuir parameters along with correlation coefficients are given in Tables 2 and 3, respectively. The correlation coefficients showed that in general, the Langmuir model fitted the results better than the Freundlich model as can be seen from Fig. 6. The monolayer adsorption capacity (Q^0), as calculated from non-linear Langmuir isotherms, for Cr(III) was three times higher for activated carbon fabric cloth than activated carbon prepared by coconut shell fibers (ATFAC). Activated carbon fibers only have micropores, which are directly accessible from the external surface of the fiber and therefore the various species of Cr(III) reach the adsorption sites through these micropores without any additional diffusion resistance of macropores. Also the activated carbon fibers (ACFs) have a high carbon content and preferentially adsorb Cr(III). Surface area is not the only criteria and other factors such as precipitation, surface complexation, and ion exchange also play an important role in the adsorption of Cr(III) on the developed adsorbents.

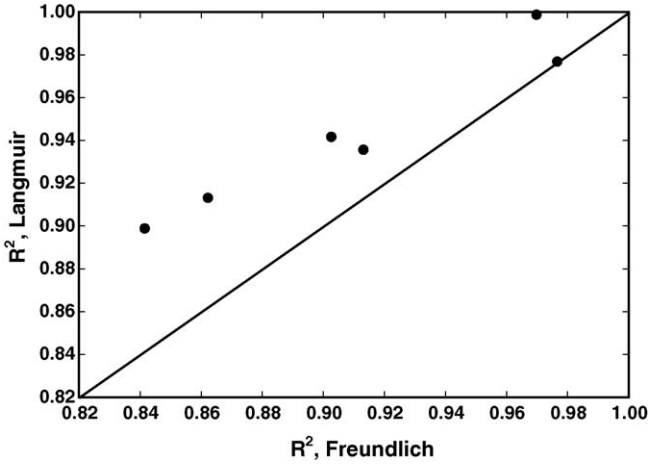

Fig. 6. Comparative evaluation of Langmuir and Freundlich regression coefficients for Cr(III) removal on ATFAC and ACF.

The essential characteristic of a Langmuir isotherm can be expressed in terms of a dimensionless constant separation factor, R_L [47–49,2,35–38] on different systems as given by Eq. (7).

$$R_L = \frac{1}{1 + bC_0} \tag{7}$$

where b is the Langmuir constant, C_0 the initial concentration, and R_L indicates the shape of the isotherm as given in Scheme 1.

Table 3
Langmuir isotherm constants for Cr(III) adsorption on FAC and ACF at different temperatures

Types of carbons	10 °C			25 °C			40 °C		
	Q^0 (mg/g)	b (l/mg)	R^2	Q^0 (mg/g)	b (l/mg)	R^2	Q^0 (mg/g)	b (l/mg)	R^2
ATFAC	10.97	0.0505	0.9356	12.23	0.0361	0.9768	16.10	0.0442	0.9987
ACF	36.05	0.0371	0.9416	39.56	0.0368	0.9131	40.29	0.0439	0.8988

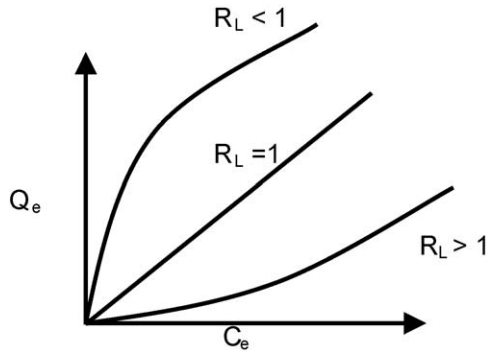

Scheme 1.

Types of equilibrium isotherms are related with the R_L values as

$R_L > 1$	Unfavorable
$R_L = 1$	Linear
$0 < R_L < 1$	Favorable
$R_L = 0$	Irreversible

The dimensionless separation factor, R_L was determined at different temperatures, particle sizes and adsorbent doses in the broad concentration range. The values of R_L at different particle sizes, adsorbent doses and temperatures were found to be less than 1 and greater than 0 indicating the favorable adsorption of Cr(III) on both of the adsorbents used for Cr(III) removal (data omitted for brevity). The degree of favorability is generally related to the irreversibility of the system giving a qualitative assessment of the carbon–chromium and cloth–carbon interactions. The degrees tended towards zero (the completely ideal irreversible case) rather than unity, which represents a completely reversible case.

3.3. Dynamic studies

The effect of amount of adsorbent on the rate of uptake of Cr(III) was carried out at 0.5, 1, and 2 g. The uptake increased with increase in amount of the adsorbent material (figure omitted for brevity). There is a substantial increase in the adsorption when carbon dosage increases from 0.5 to 1 g, while the increase on introducing additional 1 g/l of carbon is not so significant. Keeping this in view, the amount of carbon has been kept 2 g/l in all the subsequent kinetic studies. Further the half-life of the process (t_{50}) decreases with increasing amount of adsorbent, confirming that the rate of adsorption is dependent on the amount of carbon. Preliminary investigations on the rate of uptake of Cr(III) on activated carbons indicated that the processes are quite rapid and typically 40–50% of the ultimate adsorption occurs within the first hour of contact. This adsorption subsequently gives way to a very slow approach to equilibrium and in 48 h, saturation is reached.

The kinetics of removal of Cr(III) has been further studied at different adsorbate concentrations, viz., 25, 50, and 100 mg/l and temperatures, viz., 10, 25, and 40 °C and the same is presented in Figs. 7 and 8 for ATFAC and ACF, respectively.

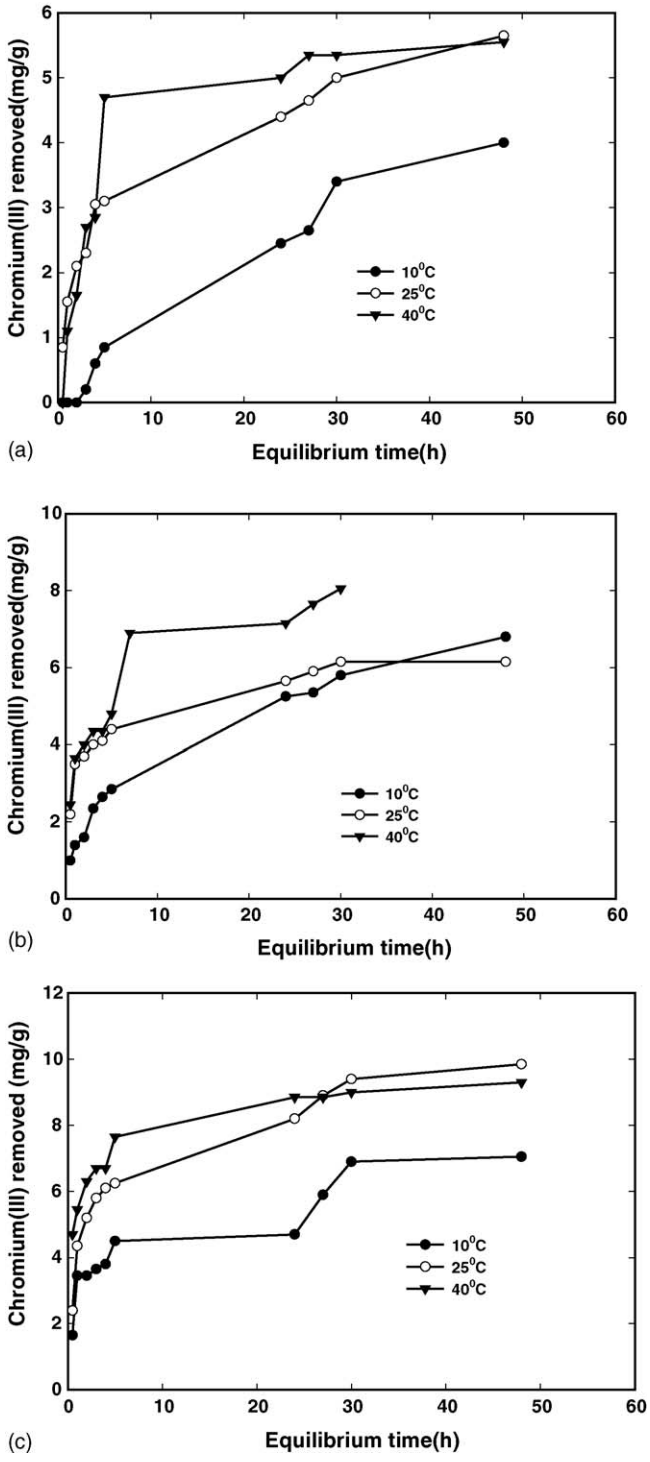

Fig. 7. Effect of contact time on the rate of adsorption of Cr(III) by ATFAC at different temperatures and at optimum pH, and adsorbate concentration of (a) 25 mg/l, (b) 50 mg/l, and (c) 100 mg/l.

The extent of adsorption of Cr(III) and its rate of removal on ATFAC, and ACF are found to increase with temperature (Table 4), conforming the process to be endothermic in nature. Also, the amount of Cr(III) removed in the first hour of contact increases with the increase in temperature. Further the uptake of Cr(III) on both the adsorbents, i.e. ATFAC and ACF increases

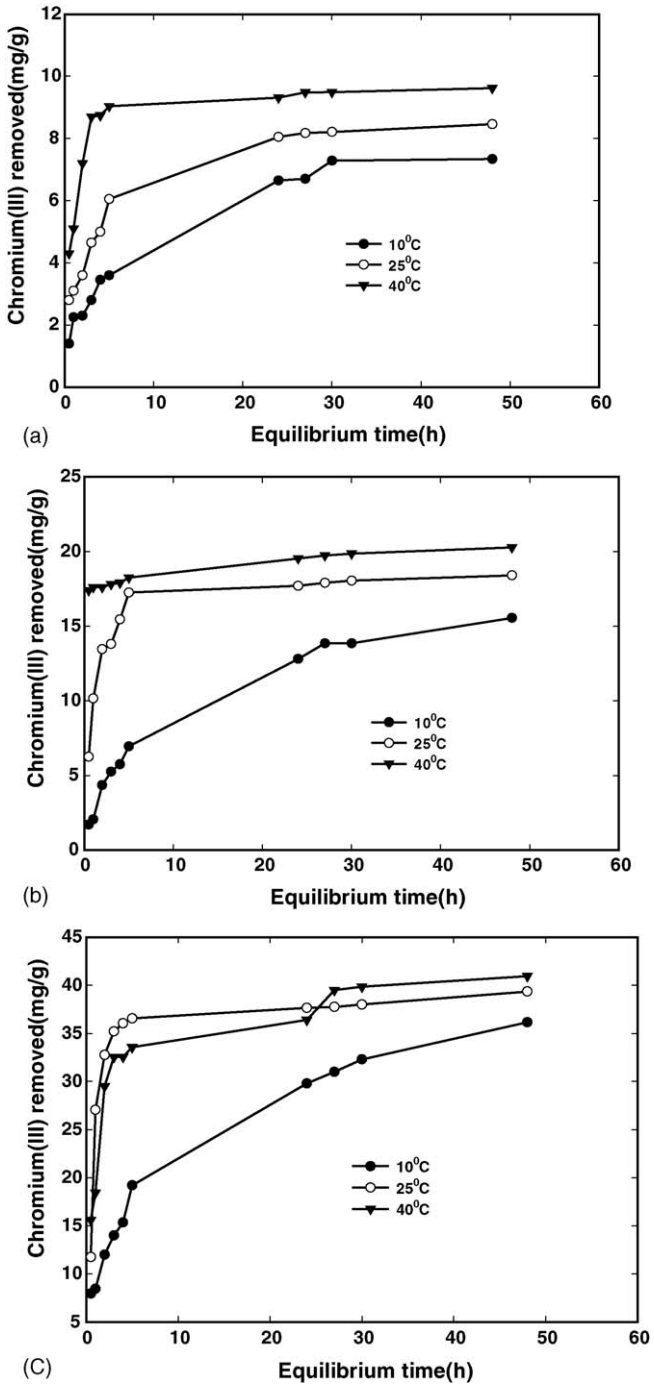

Fig. 8. Effect of contact time on the rate of adsorption of Cr(III) by ACF at different temperatures and at optimum pH, and adsorbate concentration of (a) 25 mg/l, (b) 50 mg/l, and (c) 100 mg/l.

with increase in adsorbate concentrations. Similar to the effect of temperature the removal also increases in the first hour of contact (Table 4). No correlation was found between the half-life of the adsorption process (t_{50}) and temperature/adsorbate concentration.

In order to interpret the experimental data, it is necessary to identify the step that governs the overall removal rate in the adsorption process. First-order and second-order kinetic models were tested to fit the experimental data obtained from Cr(III) adsorption. Moreover, the determination of a good fitting model could allow further water treatment process designing.

Table 4
Effect of temperatures and concentrations on the rate of uptake of Cr(III) on ATFAC and ACF (initial concentration of Cr(III) = 50 mg/l)

Adsorbents/ concentrations	Temperature (°C)	Amount adsorbed in first hour (mg/g)	Amount adsorbed as obtained experimentally
ACF (25 mg/l)	10	2.25	7.34
	25	3.10	8.46
	40	5.10	9.62
ACF (50 mg/l)	10	2.05	15.55
	25	10.15	18.05
	40	17.6	20.27
ACF (100 mg/l)	10	8.45	36.15
	25	27.05	39.35
	40	18.45	40.95
ATFAC (25 mg/l)	10	–	4.00
	25	1.55	5.65
	40	1.10	5.55
ATFAC (50 mg/l)	10	1.40	6.80
	25	3.50	6.15
	40	3.65	8.05
ATFAC (100 mg/l)	10	3.45	7.05
	25	4.35	9.80
	40	5.47	9.30

3.3.1. Pseudo-first-order kinetic model

A simple kinetic model that describes the process of adsorption is the pseudo-first-order equation as suggested by Lagergen [50] and further cited by Ho et al. [51] and Ho [52].

$$\frac{dq_t}{dt} = k_1(q_e - q_t) \tag{8}$$

where k_1 (min^{-1}) is the first-order rate constant of adsorption, q_e the amount adsorbed at equilibrium, and q_t is the amount of chromium adsorbed at time 't'.

Integrating Eq. (1) with the initial condition $q_t = 0$ at $t = 0$, we get

$$\ln\left(\frac{q_e - q_t}{q_e}\right) = -k_1 t \tag{9}$$

or

$$\log(q_e - q_t) = \log q_e - \frac{k_1}{2.303}t \quad \text{(linear form)} \tag{10}$$

or

$$q_t = q_e(1 - e^{-k_1 t}) \quad \text{(non-linear form)} \tag{11}$$

In most of the cases, the first-order equation of Lagergren did not apply throughout the complete range of contact time and is generally applicable over the initial 20–30 min of the sorption process. The plots of $\log(q_e - q_t)$ versus "time" (Fig. 9) deviated

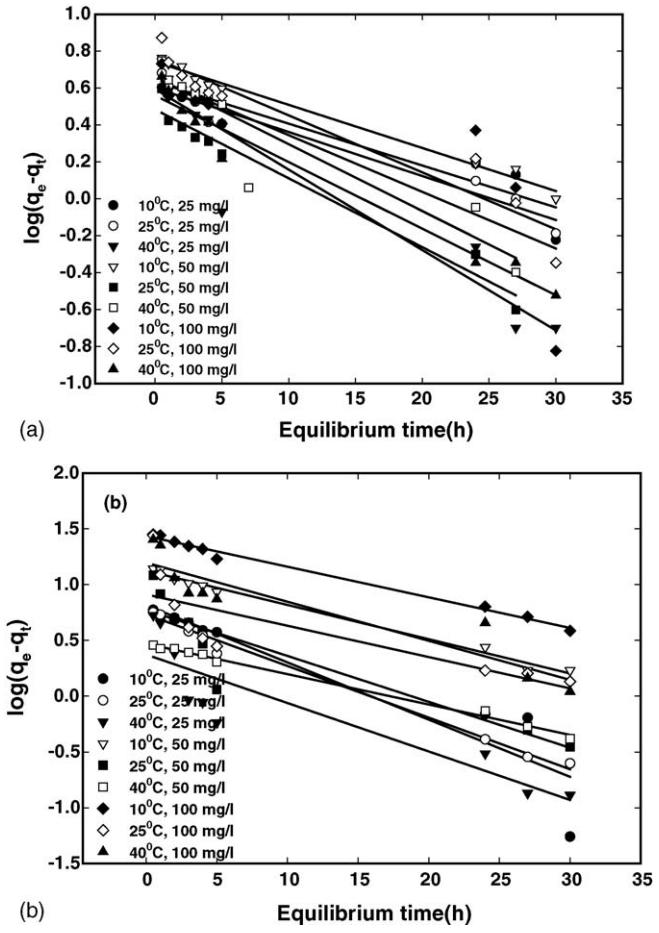

Fig. 9. Lagergren plots for the adsorption of Cr(III) on (a) ATFAC and (b) ACF at optimum pH, at different temperatures and adsorbate concentrations.

considerably from the theoretical data after a short period. The slops and intercepts as calculated from the plots were used to determine k_1 (first-order rate constant) and equilibrium capacity (q_e). The q_e values as calculated from the plots are lower than the experimental one. The values of rate constant, k_1 and q_e together with regression coefficients are provided in Table 5. Therefore, it may be concluded that chromium-adsorbent systems do not follow a first-order rate equation.

3.3.2. Pseudo-second-order kinetic model

The kinetics of chromium-adsorbent systems can be represented as

$$S + M \underset{k_2'}{\overset{k_2}{\rightleftharpoons}} SM$$

where S is an active site occupied on the adsorbent (ATFAC/ACF), M a free ion (chromium in the present study) in solution, SM represents a chromium ion bound to ATFAC/ACF, and k_2 and k_2' are the adsorption and desorption rate constants, respectively. The kinetic equation for the adsorption process was developed [53–55] and can be written as

$$\frac{d(S)_t}{dt} = k_2[(S)_0 - (S)_t]^2 \quad (12)$$

where $[S]_0$ and $[S]_t$ are the number of active sites on the adsorbent at initial time $t = 0$ and t, respectively. It is considered that sorption capacity is directly proportional to the number of active sites occupied on activated carbon/activated fabric cloth; this can be written as

$$\frac{dq_t}{dt} = k_2(q_e - q_t)^2 \quad (13)$$

where k_2 (g mg^{-1} h^{-1}) is the rate constant of pseudo-second-order adsorption, q_e the amount adsorbed at equilibrium, and q_t is the amount of chromium adsorbed at time 't'.

Separating the variables of Eq. (13)

$$\frac{dq_t}{(q_e - q_t)^2} = k_2\, dt \quad (14)$$

Integrating Eq. (14), considering that $q_0 = 0$ when $t = 0$ and that $q_t = q_t$ when $t = t$, results in the expression

$$\frac{1}{(q_e - q_t)^2} = \frac{1}{q_e} + k_2 t \quad (15)$$

Re-arranging Eq. (15)

$$q_t = \frac{t}{(1/(k_2 q_e^2)) + (t/q_e)} \quad (16)$$

Table 5
Pseudo-first-order kinetic parameters for the adsorption of Cr(III) on ATFAC and ACF

Initial concentration (mg/l)	Temperature (°C)	FAC				ACF			
		k_1 (min^{-1})	$q_{e(Exp)}$ (mg/g)	$q_{e(Cal)}$ (mg/g)	R^2	k_1 (min^{-1})	$q_{e(Exp)}$ (mg/g)	$q_{e(Cal)}$ (mg/g)	R^2
25	10	3.12	4.00	4.30	0.9207	7.08	7.34	6.53	0.8660
	25	3.30	5.65	3.98	0.9515	6.36	8.46	5.41	0.9908
	40	8.02	5.55	3.92	0.8867	5.94	9.62	2.36	0.7989
50	10	3.21	6.80	5.52	0.9877	4.14	15.55	13.30	0.9896
	25	5.14	6.15	3.05	0.9642	5.7	18.05	5.91	0.8298
	40	5.00	8.05	4.55	0.8627	3.78	20.27	2.95	0.9940
100	10	4.26	7.05	4.48	0.6590	3.72	36.15	27.23	0.9908
	25	4.26	9.80	5.76	0.9197	3.90	39.35	8.16	0.6274
	40	4.98	9.30	3.63	0.9682	4.86	40.95	15.73	0.8474

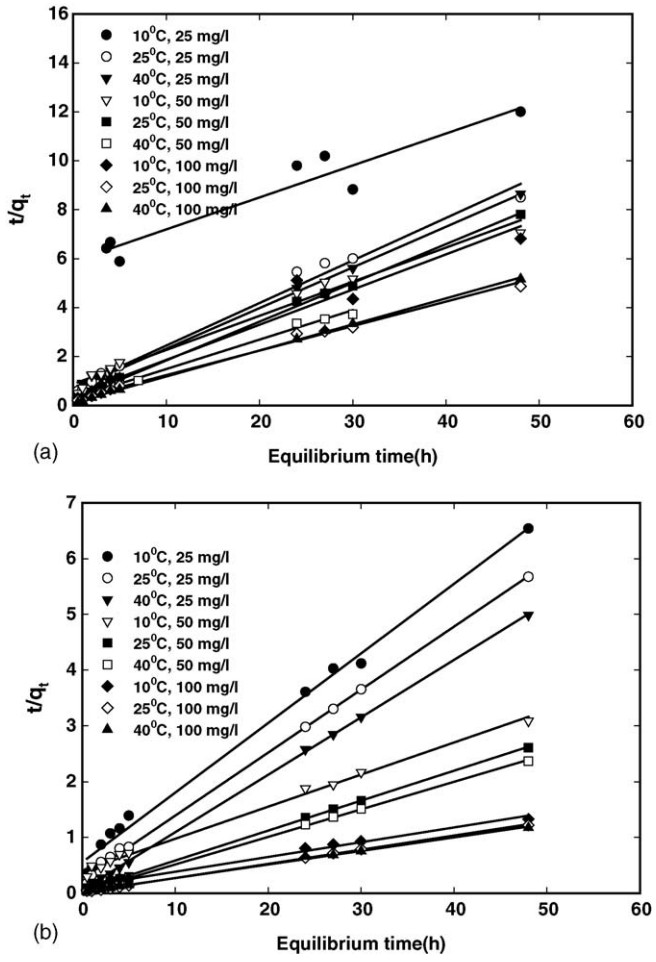

Fig. 10. Pseudo-second-order kinetic plots for the adsorption of Cr(III) on (a) ATFAC and (b) ACF at optimum pH, at different temperatures and different initial concentrations of adsorbate.

or

$$\frac{t}{q_t} = \frac{1}{k_2 q_e^2} + \frac{t}{q_e} \tag{17}$$

The product $k_2 q_e^2$ is actually represents the initial sorption rate represented as

$$\text{Rate} = k_2 q_e^2 \tag{18}$$

Using Eq. (17), t/q_t was plotted against 't' at different adsorbate concentrations at different temperature. The second-order sorption rate constant (k_2) and q_e values were determined from slopes and intercepts of the plots (Fig. 10). The correlation coefficients (R^2) for the linear plots are superior (in most cases $\geq$0.9900). The values of q_e and k_2 are presented in Table 6. The kinetic data is better fitted by second-order rate equation (Fig. 11). Further, the experimentally q_e values were compared with the q_e values determined by pseudo-first and second-order rate kinetic models. The theoretical q_e values as calculated from pseudo-second-order kinetic model agree perfectly with the experimental q_e values (Fig. 12). This suggests that the sorption system is not a first-order reaction and that a pseudo-second-order model

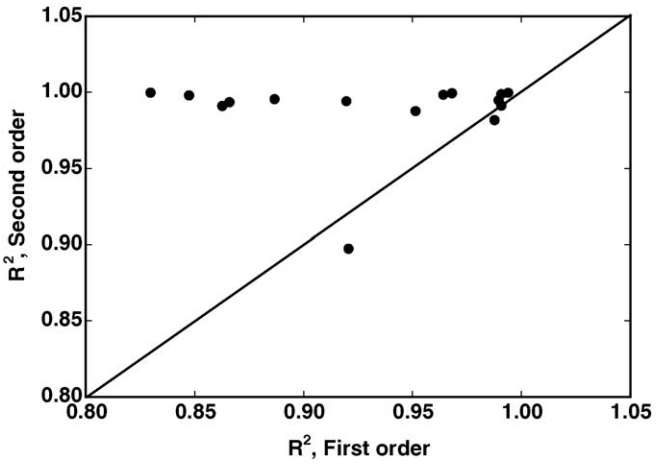

Fig. 11. Comparative evaluation of pseudo-first-order and pseudo-second-order rate equations.

can be considered. The pseudo-second-order model is based on the assumption that the rate-limiting step may be a chemical sorption involving valance forces through sharing or exchange of electrons between adsorbent and adsorbate. It provides the best correlation of the data. These two models do not provide a definite mechanism, therefore another simplified model was tested.

The mathematical treatment of Boyd et al. [56] and Reichenberg [57] distinguishes between diffusion in particle, film diffusion and a mass action-controlled exchange mechanism. This treatment laid the foundation of sorption/ion exchange kinetics.

Three consecutive steps which occur in the adsorption of an adsorbate by a porous adsorbent are:

1. transport of the adsorbate to the external surface of the adsorbent (film diffusion);
2. transport of the adsorbate within the pores of the adsorbent (particle diffusion);

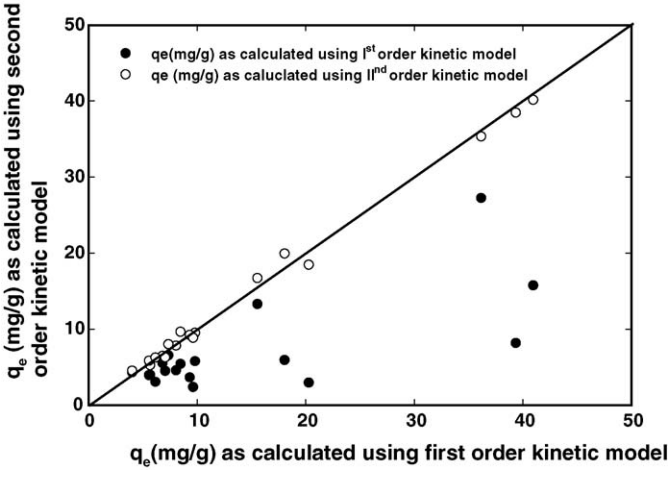

Fig. 12. Correlation between experiment q_e, and calculated q_e using pseudo-first and second-order kinetic models.

Table 6
Pseudo-second-order kinetic parameters for the adsorption of Cr(III) on ATFAC and ACF

Initial concentration (mg/l)	Temperature (°C)	ATFAC				ACF			
		$k_2 \times 10^{-2}$ (g mg^{-1} h^{-1})	$q_{e(Exp)}$ (mg/g)	$q_{e(Cal)}$ (mg/g)	R^2	$k_2 \times 10^{-2}$ (g mg^{-1} h^{-1})	$q_{e(Exp)}$ (mg/g)	$q_{e(Cal)}$ (mg/g)	R^2
25	10	1.26	4.00	4.51	0.8973	2.83	7.34	7.99	0.9935
	25	6.23	5.65	5.24	0.9876	0.18	8.46	9.64	0.9988
	40	5.79	5.55	5.82	0.9955	4.95	9.62	8.83	0.9998
50	10	3.14	6.80	6.46	0.9817	93.97	15.55	16.69	0.9947
	25	0.11	6.15	6.25	0.9983	0.17	18.05	19.92	0.9997
	40	5.96	8.05	7.82	0.9910	6.81	20.27	18.45	0.9996
100	10	8.16	7.05	6.27	0.9597	75.01	36.15	35.33	0.9912
	25	5.59	9.80	9.49	0.9941	5.49	39.35	38.46	0.9993
	40	0.11	9.30	9.21	0.9993	2.68	40.95	40.16	0.9979

3. adsorption of the adsorbate on the exterior surface of the adsorbent.

Process (3) is very rapid and does not represent the rate-determining step in the uptake of adsorbate [39]. Three distinct cases occur for the remaining two steps in the overall transport:

case I: external transport > internal transport;
case II: external transport < internal transport;
case III: external transport ≈ internal transport.

In cases I and II, the rate is governed by film and particle diffusion, respectively. In case III, the transport of ions to the boundary may not be possible at a significant rate, thereby, leading to the formation of a liquid film with a concentration gradient surrounding the sorbent particles. External transport is usually the rate-limiting step in systems, which have (a) poor mixing, (b) dilute concentration of adsorbate, (c) small particle size, and (d) high affinity of adsorbate for adsorbent.

In contrast, the intra-particle step limits the overall transfer for those systems that have (a) high concentration of adsorbate, (b) good mixing, (c) large particle size of adsorbent, and (d) low affinity of adsorbate for adsorbent.

Kinetic data obtained in this work were analyzed by applying the Reichenberg [57], and Helffrich [58] mathematical models using Eqs. (19)–(24).

$$F = 1 - \frac{6}{\pi^2}\sum_{n=1}^{\infty}\frac{1}{n^2}\left[\frac{-D_i t\pi^2 n^2}{r_0^2}\right] \tag{19}$$

or

$$F = 1 - \frac{6}{\pi^2}\sum_{n=1}^{\infty}\frac{1}{n^2}\exp[-n^2 Bt] \tag{20}$$

where F is the fractional attainment of equilibrium at time 't' and is obtained by the expression

$$F = \frac{Q_t}{Q^0} \tag{21}$$

where Q_t is the amount of adsorbate taken up at time 't' and Q^0 is the maximum equilibrium uptake and

$$B = \frac{\pi^2 D_i}{r_o^2} = \text{time constant} \tag{22}$$

where D_i is the effective diffusion coefficient of ion in the adsorbent phase, r_o the radius of the adsorbent particle, assumed to be spherical, and n is an integer that defines the infinite series solution. Bt values were obtained for each observed value of F from Reichenberg's table [57] at different temperatures and concentrations. The linearity test of Bt versus time plots was

Table 7
Thermodynamic parameters of activation

Adsorbents	Effective diffusion coefficient, D_i (m^2 s^{-1})			Pre-exponential factor (D_0) (m^2 s^{-1})	Energy of activation (E_a) (kJ mol^{-1})	Entropy of activation ($\Delta S^{\#}$) (J K^{-1} mol^{-1})
	10 °C	25 °C	40 °C			
ATFAC (25 mg/l)	746.82×10^{-16}	118.51×10^{-16}	276.93×10^{-16}	9.91×10^{-19}	11.04	0.11
ATFAC (50 mg/l)	111.84×10^{-16}	213.42×10^{-16}	167.95×10^{-16}	1.04×10^{-12}	4.49	4.02
ATFAC (100 mg/l)	172.77×10^{-16}	165.08×10^{-16}	219.06×10^{-16}	0.18×10^{-14}	2.47	2.23
ACF (25 mg/l)	267.39×10^{-16}	254.06×10^{-10}	253.04×10^{-16}	1.48×10^{-14}	5.95	2.82
ACF (50 mg/l)	156.29×10^{-16}	160.17×10^{-10}	229.34×10^{-16}	0.76×10^{-14}	4.02	2.63
ACF (100 mg/l)	139.62×10^{-16}	162.30×10^{-10}	196.19×10^{-16}	0.48×10^{-14}	3.61	2.50

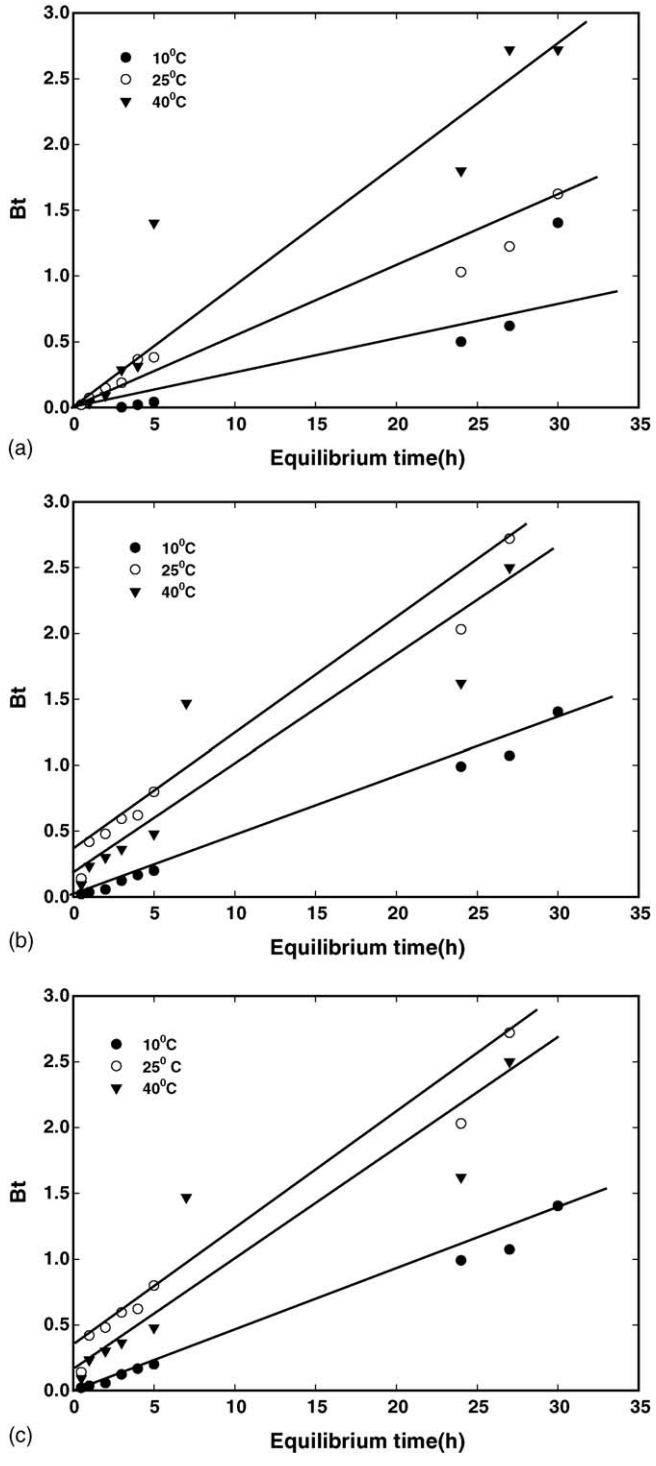

Fig. 13. *Bt* vs. time plots for Cr(III) adsorption on ATFAC at (a) 25 mg/l, (b) 50 mg/l, and (c) 100 mg/l.

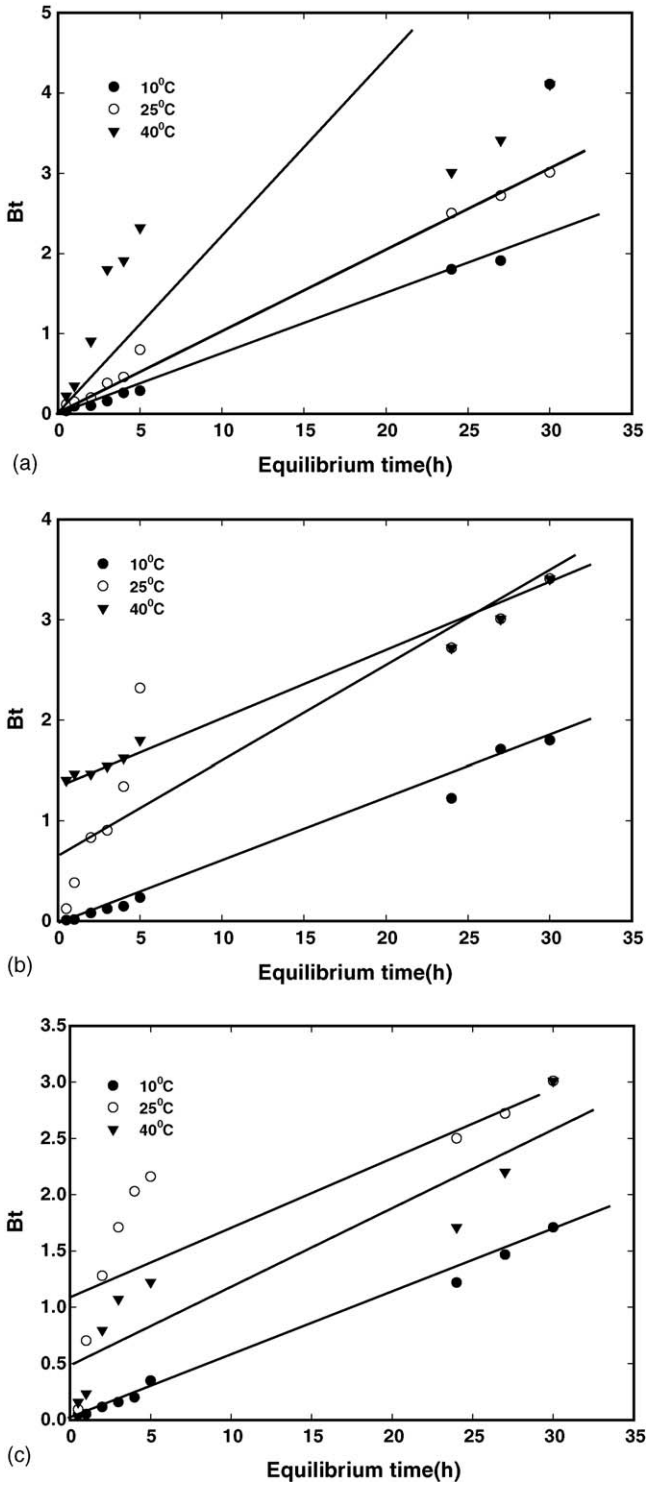

Fig. 14. *Bt* vs. time plots for Cr(III) adsorption on ACF at (a) 25 mg/l, (b) 50 mg/l, and (c) 100 mg/l.

employed to distinguish between the film diffusion and particle diffusion controlled adsorption. If the plot of *Bt* versus time (having slope *B*) is a straight line passing through the origin, then the adsorption rate is governed by particle diffusion mechanism otherwise it is governed by film diffusion. The results of ATFAC and ACF at different concentrations and temperatures are plotted in Figs. 13 and 14 (other figures omitted for brevity). It is interesting to note that at 10, 25, and 40 °C and low concentrations, i.e. ≤ 25 mg/l for ATFAC, ACF the *Bt* versus time plots are linear and passes through the origin indicating the particle diffusion mechanism is the rate controlling step. Further at concentration ≥25 mg/l and at low temperatures ≤10 °C, the plots are linear and pass through the origin indicating the particle diffusion mechanism at these conditions for both ATFAC

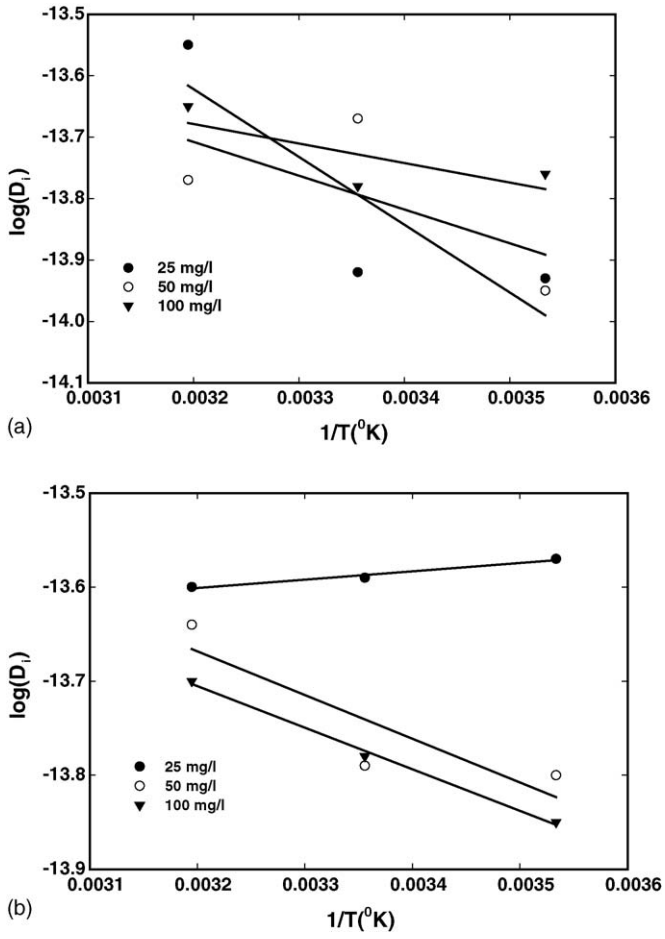

Fig. 15. $\log(D_i)$ vs. $1/T$ plots for Cr(III) adsorption on (a) ATFAC and (b) ACF.

and ACF. At high temperatures (>10 °C) and high concentrations (>25 mg/l) the plots are liner but do not pass through the origin confirmed that the film diffusion mechanism control the rate of the reaction (Figs. 13 and 14).

The effective diffusion coefficients were estimated from the slopes of the Bt plots using Eq. (19). The effective diffusion coefficients as estimated from Fig. 15 at different temperatures are given in Table 7. No correlation was observed between temperatures and effective diffusion coefficients. The increased mobility of ions and a decrease in retarding forces acting on the diffusing ion results in the increase of D_i with temperature in some cases. The energy of activation, E_a, the entropy of activation, $\Delta S^{\#}$, and pre-exponential factor, D_0, analogous to the Arrhenius frequency factor, were also evaluated using Eqs. (23) and (24) and are given in Table 7.

$$D_i = D_0 \exp\left[-\frac{E_a}{RT}\right] \quad (23)$$

$$D_0 = 2.72d^2\frac{kT}{h} \exp\left[\frac{\Delta S^{\#}}{R}\right] \quad (24)$$

where k is the Boltzmann constant, h the Planck constant, R the gas constant, and d is the distance between two active sites of the adsorbent. The positive $\Delta S^{\#}$ values obtained for the adsorption of Cr(III) on ATFAC and ACF are common in metal adsorption.

4. Conclusions

The agricultural waste material, i.e. coconut shell fibers was converted into low cost activated carbon (ATFAC) successfully. The carbon together with the activated carbon fabric cloth were characterized and utilized for the removal of Cr(III)

Table 8
Adsorption capacities of the developed adsorbents vis-à-vis other adsorbents for the removal of Cr(III)

Activated carbons/adsorbents	Adsorption capacity (mg/gram)	References
ATFAC	12.23	This study
ACF	39.56	
Activated carbon, GAC-S	13.31	[44]
Activated carbon, GAC-E	10.52	
Activated carbon, ACF-307	7.08	
Activated carbon, ACF-310	3.52	
Carbon F	7.33	[43]
Carbon F10	10.67	
Carbon F120	19.23	
Chrome sludge	24.0	[59]
Pinus pinaster bark	19.45	[60]
Rice straw	15.6	[61]
Sun flower stalks	25.07	[62]
Blast furnace sludge	9.55	[63]
Treated *Pinus sylvestris* bark	9.77	[64]
Untreated *Pinus sylvestris* bark	8.69	
Moss	15.1	[65]
Moss-tannery waste	13.1	
Sargassum	38	[66]
Rhizopus arrhizus	31	[67]
Ecklonia biomass	34.1	[68]
Biogas residual slurry	7.8	[69]
Activated carbon	2.7	[70]
Activated carbon oxidized with HNO_3	25.3	
Activated carbon oxidized with HNO_3 and heated at 873 °K in a N_2 flow for 2 h	0.2	
Natural moss	18.9	[71]
Composite alginate–goethite beads	25.2	[72]
Carbons prepared from co-mingled natural organic wastes	56.68	[73]
Norit activated carbon post-oxidized with 1 M HNO_3	53.04	
Expanded perlite	0.73	[74]
Alginate beads	0.14	[75]
Impregnated with microemulsion	85.59	[76]
Aminated polyacrylonitrile fibers	~5.0	[23]
Wine processing waste sludge	13.45	[42]
Brown seaweed (*Turbinaria* spp.)	31	[16]
Peat	22.36	[77]

from water/wastewater in the broad range of concentrations (1–100 mg/l). The results are very promising. Both equilibrium and kinetic studies were performed in batch due to its simplicity to determine various parameters necessary to establish the fixed bed reactors. The optimum pH was 5.0. The sorption data are better fitted by Langmuir adsorption isotherm model than Freundlich model. The monolayer adsorption capacity (Q^0) as calculated using Langmuir adsorption isotherm of ATFAC and ACF increased with increase in temperature conforming endothermic nature of the process. Sorption capacities are comparable to most of the adsorbents used for Cr(III) removal from water/wastewater (Table 8). Further, adsorption of Cr(III) was more on ACF than ATFAC.

The rate of the adsorption is governed by pseudo-second-order rate equation. Further the adsorption of Cr(III) is controlled by particle diffusion mechanism at temperatures $\leq$10 °C and adsorbate concentrations $\leq$25 mg/l. It is concluded that the coconut shell fibers commodity group will be benefited from this research because it will add value to surplus by-products. Carbon users would also be benefited because it offers a viable alternative to coal based activated carbons, Thus, the studies presented revealed that the derived low cost activated carbon could be fruitfully employed as adsorbent for the removal of chromium from wastewater with out any sludge production.

Acknowledgements

The authors are thankful to the Director, Industrial Toxicology Research Centre, Lucknow, for providing all necessary facilities for this work and consistent encouragement and guidance throughout this work. The authors are also very much thankful to Professor Vicente Gomez Serrano, Universidad Extremadura, Spain, for carrying out the surface characterization of activated carbon (ATFAC).

References

[1] B.M. Braukman, Industrial solutions amenable to biosorption, in: B. Volesky (Ed.), Biosorption of Heavy Metals, CRC Press, USA, 1990, pp. 51–64.
[2] D. Mohan, K.P. Singh, V.K. Singh, Removal of hexavalent chromium from aqueous solution using low-cost activated carbons derived from agricultural waste materials and activated carbon fabric cloth, Ind. Eng. Chem. Res. (ACS) 44 (2005) 1027–1042.
[3] G. Tiravanti, D. Petruzzelli, R. Passino, Pretreatment of tannery wastewaters by an ion exchange process for Cr(III) removal and recovery, Water Sci. Technol. 36 (1997) 197–207.
[4] S. Rengaraj, C.K. Joo, Y. Kim, J. Yi, Kinetics of removal of chromium from water and electronic process wastewater by ion exchange resins: 1200H, 1500H and IRN97H, J. Hazard. Mater. 102 (2003) 257–275.
[5] D. Petruzzelli, R. Passino, G. Tiravanti, Ion exchange process for chromium removal and recovery from tannery wastes, Ind. Eng. Chem. Res. 34 (1995) 2612–2617.
[6] J.C. Seaman, P.M. Bertsch, L. Schwallie, In situ Cr(VI) reduction within coarse-textured, oxide-coated soil and aquifer systems using Fe(II) solutions, Environ. Sci. Technol. 33 (1999) 938–944.
[7] X. Zhou, T. Korenaga, T. Takahashi, T. Moriwake, S. Shinoda, A process monitoring/controlling system for the treatment of wastewater containing chromium (VI), Water Res. 27 (1993) 1049–1054.
[8] H. Shaalan, M. Sorour, S. Tewfik, Simulation and optimization of a membrane system for chromium recovery from tanning wastes, Desalination 14 (2001) 315–324.
[9] C.A. Kozlowski, W. Walkowiak, Removal of chromium (VI) from aqueous solutions by polymer inclusion membranes, Water Res. 36 (2002) 4870–4876.
[10] N. Kongsricharoern, C. Polprasert, Chromium removal by a bipolar electrochemical precipitation process, Water Sci. Technol. 34 (1996) 109–116.
[11] J.J. Testa, M.A. Grela, M.I. Litter, Heterogeneous photocatalytic reduction of chromium (III) over TiO_2 particles in the presence of oxalate: involvement of Cr(VI) species, Environ. Sci. Technol. 38 (2004) 1589–1594.
[12] S.K. Srivastava, V.K. Gupta, D. Mohan, Removal of lead and chromium by activated slag—a blast furnace waste, J. Environ. Eng. (ASCE) 123 (1997) 461–468.
[13] S.K. Srivastava, V.K. Gupta, D. Mohan, Kinetic parameters for the removal of lead and chromium from wastewater using activated carbon developed from fertilizer waste material, Environ. Model. Assess. 1 (1997) 281–290.
[14] V.K. Gupta, K.T. Park, S. Sharma, D. Mohan, Removal of chromium (VI) from electroplating industry wastewater using bagasse flyash—a sugar industry waste material, The Environmentalist 19 (1999) 129–136.
[15] V.K. Gupta, A.K. Shrivastava, N. Jain, Biosorption of chromium (VI) from aqueous solutions by green algae *spirogyra* species, Water Res. 35 (2001) 4079–4085.
[16] R. Arvindhan, B. Madhan, J.R. Rao, B.U. Nair, T. Ramasami, Bioaccumulation of chromium from tannery wastewater: an approach for chrome recovery and reuse, Environ. Sci. Technol. 38 (2004) 300–306.
[17] S.B. Lalvani, T. Wiltowski, A. Hubner, A. Wetson, N. Mandich, Removal of hexavalent chromium and metal cations by selective and novel carbon adsorbent, Carbon 36 (1998) 1219–1226.
[18] C.P. Hung, M.H. Wu, The removal of chromium (VI) from dilute solution by activated carbon, Water Res. 11 (1977) 673–679.
[19] R. Leyva-Ramos, L. Fuentes-Rubio, R.M. Guerrero-Coronado, J. Mendoza-Barron, Adsorption of Cr(III) from aqueous solutions onto activated carbon, J. Chem. Technol. Biotechnol. 62 (1995) 64–67.
[20] R. Leyva-Ramos, J. Martinez, R. Guerrero-Coronado, Adsorption of Cr(IV) from aqueous solutions onto activated carbon, Water Sci. Technol. 30 (1994) 191–197.
[21] M.H. Liu, H. Zhang, X.S. Zhang, Y. Deng, W.G. Lu, H.Y. Zhan, Removal and recovery of chromium (III) from aqueous solutions by spheroidal cellulose adsorbent, Water Environ. Res. 73 (2001) 322–328.
[22] Z. Reddad, C. Gerenete, Y. Andres, P. LeCloeiric, Mechanism of Cr(III) and Cr(VI) removal from aqueous solutions by sugar beet pulp, Environ. Technol. 24 (2003) 257–264.
[23] S. Deng, R. Bai, Removal of trivalent and hexavalent chromium with aminated polyacrylonitrile fibers: performance and mechanism, Water Res. 38 (2004) 2424–2432.
[24] J.P. Ibáñez, Y. Umetsu, Uptake of trivalent chromium from aqueous solutions using protonated dry alginate beads, Hydrometallurgy 72 (2004) 327–334.
[25] C. Selomulya, V. Meeyoo, R. Amal, Mechanisms of Cr(VI) removal from water by various types of activated carbons, J. Chem. Technol. Biotechnol. 74 (1999) 111–122.
[26] V.M. Boddu, K. Abburi, J.L. Talbott, E.D. Smith, Removal of hexavalent chromium from wastewater using a new composite chitosan biosorbent, Environ. Sci. Technol. 37 (2003) 4449–4456.
[27] J. Rivera-Utrilla, I.B. Toledo, M.A. Ferro-Garcia, C. Moreno-Satilla, Biosorption of Pb(II), Cd(II), and Cr(VI) on activated carbon from aqueous solutions, Carbon 41 (2003) 323–330.
[28] V.K. Gupta, I. Ali, Removal of lead and chromium from wastewater using bagasse fly ash—a sugar industry waste, J. Colloid Interface Sci. 271 (2004) 321–328.
[29] V.K. Gupta, M. Gupta, S. Sharma, Process development for the removal of lead and chromium from aqueous solutions using red mud—an aluminium industry waste, Water Res. 35 (2001) 1125–1134.

[30] S. Babel, S.T.A. Kurniawan, Cr(VI) removal from synthetic wastewater using coconut shell charcoal and commercial activated carbon modified with oxidizing agents and/or chitosan, Chemosphere 54 (2004) 951–967.
[31] C. Covarrubias, R. Arriagada, J. Yanez, R. Garcia, M. Angelica, S.D. Barros, P. Arroyo, E.F. Sousa-Aguiar, Removal of chromium (III) from tannery effluents, using a system of packed columns of zeolita and activated carbon, J. Chem. Technol. Biotechnol. 80 (2005) 899–908.
[32] S.J.T. Pollard, G.D. Fowler, C.J. Sollars, R. Perry, Low cost adsorbents for waste and wastewater treatment: a review, Sci. Total Environ. 116 (1992) 31–52.
[33] L.R. Rodovic, C. Moreno-Castilla, J. Rivera-Utrilla, Carbon materials as adsorbents in aqueous solutions, in: L.R. Radovic (Ed.), Chemistry and Physics of Carbon, vol. 27, Marcel Dekker, New York, 2000.
[34] V.K. Gupta, I. Ali, Adsorbents for water treatment: development of low cost alternatives to carbon for the updated, in: Somasundaran (Ed.), Encyclopedia of Surface and Colloid Science, Marcel Dekker, 2003, pp. 1–34.
[35] D. Mohan, K.P. Singh, S. Sinha, D. Gosh, Removal of pyridine derivatives from aqueous solution by activated carbons developed from agricultural waste materials, Carbon 43 (2005) 1680–1693.
[36] D. Mohan, K.P. Singh, D. Gosh, Removal of α-picoline, β-picoline, and γ-picoline from synthetic wastewater using low cost activated carbons derived from coconut shell fibers, Environ. Sci. Technol. 39 (2005) 5076–5086.
[37] D. Mohan, K.P. Singh, S. Sinha, D. Gosh, Removal of pyridine from aqueous solution using low cost activated carbon derived from agricultural waste materials, Carbon 42 (2004) 2409–2421.
[38] D. Mohan, K.P. Singh, Single and multicomponent adsorption of zinc and cadmium from wastewater using activated carbon derived from bagasse—an agricultural waste material, Water Res. 36 (2002) 2302–2316.
[39] D. Mohan, S.K. Srivastava, V.K. Gupta, S. Chander, Kinetics of mercury adsorption from wastewater using activated carbon derived from fertilizer waste material, Colloids Surf. A 177 (2001) 169–181.
[40] A.I. Vogel, A Textbook of Quantitative Chemical Analysis, fifth ed., ELBS Publication, London, England, 1989.
[41] J.C. Crittenden, T.F. Speth, D.W. Hand, P.J. Luft, B. Lykins, Evaluating multicomponent competitive adsorption in fixed beds, J. Environ. Eng. (ASCE) 113 (1987) 1363.
[42] Y.-S. Li, C.-C. Liu, C.-C. Chiou, Adsorption of Cr(III) from wastewater by wine processing waste sludge, J. Colloid Interface Sci. 273 (2004) 95–101.
[43] J. Rivera-Utrilla, M. Sanchez-Polo, Adsorption of Cr(III) on ozonized activated carbon. Importance of Cpi–cation interactions, Water Res. 37 (2003) 3335–3340.
[44] D. Aggarwal, M. Goyal, R.C. Bansal, Adsorption of chromium by activated carbon from aqueous solution, Carbon 37 (1999) 1989–1997.
[45] S.-J. Park, W.-Y. Jung, Removal of chromium by activated carbon fibers plated with copper metal, Carbon Sci. 2 (2001) 15–21.
[46] C.H. Gilles, D. Smith, A.J.J. Huitson, J. Colloid Interface Sci. 47 (1974) 755.
[47] K.R. Hall, L.C. Eagleton, A. Acrivos, T. Vermeulen, Pore and solid-diffusion kinetics in fixed-bed adsorption under constant-pattern conditions, Ind. Eng. Chem. Fundam. 5 (1966) 212–223.
[48] Y.S. Ho, C.T. Huang, H.W. Huang, Equilibrium sorption isotherm for metal ions on tree fern, Process Biochem. 37 (2002) 1421–1430.
[49] T.W. Weber, R.K. Chackravorti, Pore solid diffusion models for fixed bed adsorbers, J. Am. Inst. Chem. Eng. 20 (1974) 228.
[50] S. Lagergren, About the theory of so-called adsorption of soluble substances, der Sogenannten adsorption geloster stoffe Kungliga Svenska Vetenska psalka de Miens Handlingar 24 (1898) 1–39.
[51] Y.S. Ho, D.A.J. Wase, C.F. Forster, Kinetic studies of competitive heavy metal adsorption by sphagnum moss peat, Environ. Technol. 17 (1996) 71–77.
[52] Y.S. Ho, Citation review of Lagergren kinetic rate equation on adsorption reactions, Scientometrics 59 (2004) 171–177.
[53] Y.S. Ho, G. Mckay, Sorption of dyes from aqueous solution by peat, Chem. Eng. J. 70 (1998) 115–124.
[54] Y.S. Ho, G. Mckay, Pseudo-second order model for sorption process, Process Biochem. 34 (1999) 451.
[55] Y.S. Ho, G. Mckay, The kinetics of sorption of divalent metal ions onto sphagnum moss peat, Water Res. 34 (2000) 735–742.
[56] G.E. Boyd, A.W. Adamson, L.S. Mayers, The exchange adsorption of ions from aqueous solution by organic zeolites. II. Kinetics, J. Am. Chem. Soc. 69 (1947) 2836.
[57] D. Reichenberg, Properties of ion-exchange resin in relation to their structure. III. Kinetics of exchange, J. Am. Chem. Soc. 75 (1953) 589.
[58] F. Helffrich, Ion-Exchange, McGraw-Hill, New York, 1962.
[59] K.S. Low, C.K. Lee, S.T. Owe-Wee, Removal of Cr(III) from aqueous solution using chrome sludge, Bull. Environ. Contam. Toxicol. 55 (1995) 270–275.
[60] L.A. Teles de Vasconcelos, C.G. Gonzalez Beca, Adsorption equilibria between pine bark and several ions in aqueous solution, 1. Pb(II), Eur. Water Pollut. Control 4 (1993) 41–51.
[61] W.T. Tan, N.Y. Cheong, C.K. Lee, Removal of Cr(III) from aqueous solution by coconut husk and rice straw, Pertanika 1 (1989) 764–769.
[62] G. Sun, W. Shi, Sunflower stalks as adsorbents for the removal of metals from wastewater, Ind Eng. Chem. Res. 37 (1998) 1324–1328.
[63] A. Lopez-Delgado, C. Perez, F.A. Lopez, Sorption of heavy metals on blast furnace sludge, Water Res. 32 (1998) 989–996.
[64] M.M. Alves, C.G. Gonzalez, Beca, R. Guedes de Carvalho, J.M. Castanheira, M.C. Sol Pereira, L.A.T. Vasconcelos, Chromium removal in tannery wastewaters "polishing" by *Pinus sylvestris* bark, Water Res. 27 (1993) 1333–1338.
[65] K.S. Low, C.K. Lee, S.G. Tan, Sorption of trivalent chromium from tannery waste by moss, Environ. Technol. 18 (1997) 449–454.
[66] D. Kratochvil, P. Pimental, B. Volesky, Removal of trivalent and hexavalent chromium by seaweed biosorbent, Environ. Sci. Technol. 32 (1998) 2693–2698.
[67] J.M. Tobin, The uptake of metals by *Rhizopus arrhizus* biomass, Ph.D. Thesis, McGill University, 1986.
[68] Y.-S. Yun, D. Park, Y.M. Park, B. Volesky, Biosorption of trivalent chromium on the brown seaweed biomass, Environ. Sci. Technol. 35 (2001) 4353–4358.
[69] C. Namasivayam, R.T. Yamuna, Studies on chromium (III) removal from aqueous solution by adsorption onto biogas residual slurry and its application to tannery wastewater treatment, Water Air Soil Pollut. 113 (1999) 371–384.
[70] I. Bautista-Toledo, J. Rivera-Utrilla, M.A. Ferro-García, C. Moreno-Castilla, Influence of the oxygen surface complexes of activated carbons on the adsorption of chromium ions from aqueous solutions: effect of sodium chloride and humic acid, Carbon 32 (1994) 93–100.
[71] C.K. Lee, S. Low, K.L. Kek, Removal of chromium from aqueous solution, Bioresour. Technol. 54 (1995) 183–189.
[72] N.K. Lazaridis, Ch. Charalambous, Sorptive removal of trivalent and hexavalent chromium from binary aqueous solutions by composite alginate–goethite beads, Water Res. 39 (2005) 4385–4396.
[73] S.I. Lyubchik, A.I. Lyubchik, O.L. Galushko, L.P. Tikhonova, J. Vital, I.M. Fonseca, S.B. LyubchikKinetics, Thermodynamics of the Cr(III) adsorption on the activated carbon from co-mingled wastes, Colloids Surf. A 242 (2004) 151–158.
[74] A. Chakir, J. Bessiere, K.E. Kacemi, B.A. Marouf, Comparative study of the removal of trivalent chromium from aqueous solutions by bentonite and expanded perlite, J. Hazard. Mater. 95 (2002) 29–46.
[75] M.M. Araújo, J.A. Teixeira, Trivalent chromium sorption on alginate beads, Int. Biodeterior. Biodegrad. 40 (1997) 63–74.
[76] T.N. de Castro Dantas, A.A. Dantas Neto, M.C.P. de A. Moura, E.L. Barros Neto, E. de Paiva Telemaco, Chromium adsorption by chitosan impregnated with microemulsion, Langmuir 17 (2001) 4256–4260.
[77] W. Ma, J.M. Tobin, Determination and modelling of effects of pH on peat biosorption of chromium, copper and cadmium, Biochem. Eng. J. 18 (2004) 33–40.